



Infrared interferometric imaging of the symbiotic Mira R Aquarii

Work in progress

Markus Wittkowski (ESO)

E. Humphreys, C. Paladini (ESO), G. Rau (NSF, NASA)

Picture:ESO/ M. Kornmesser

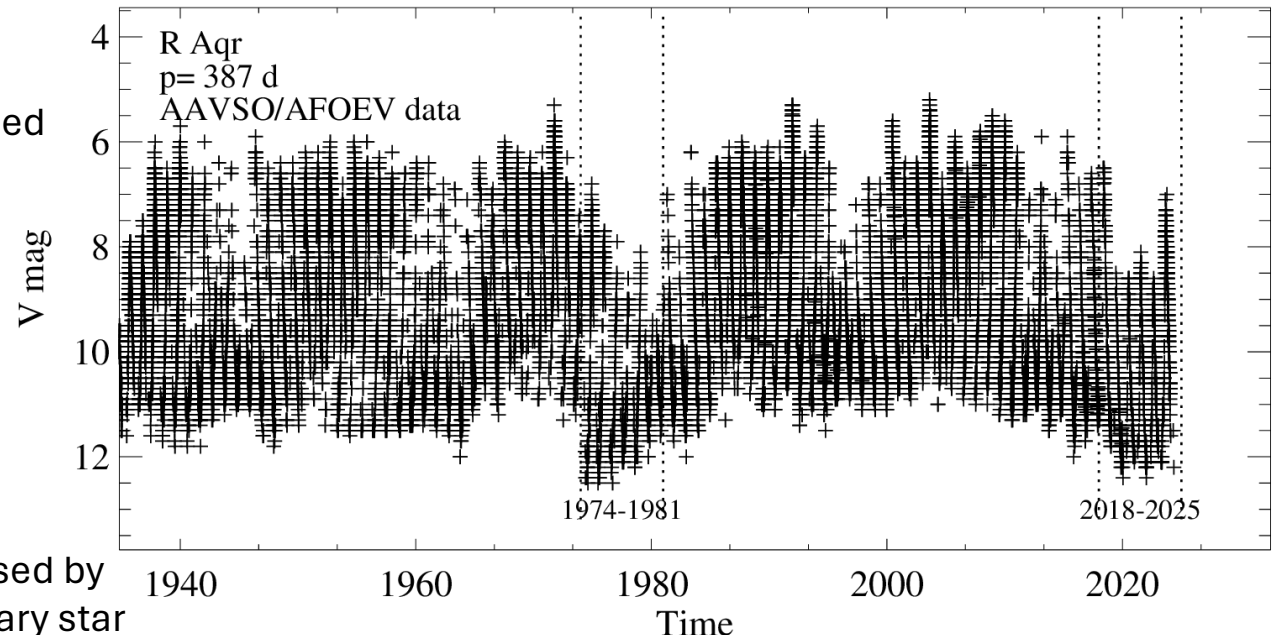
Symbiotic Mira R Aqr: Characteristics

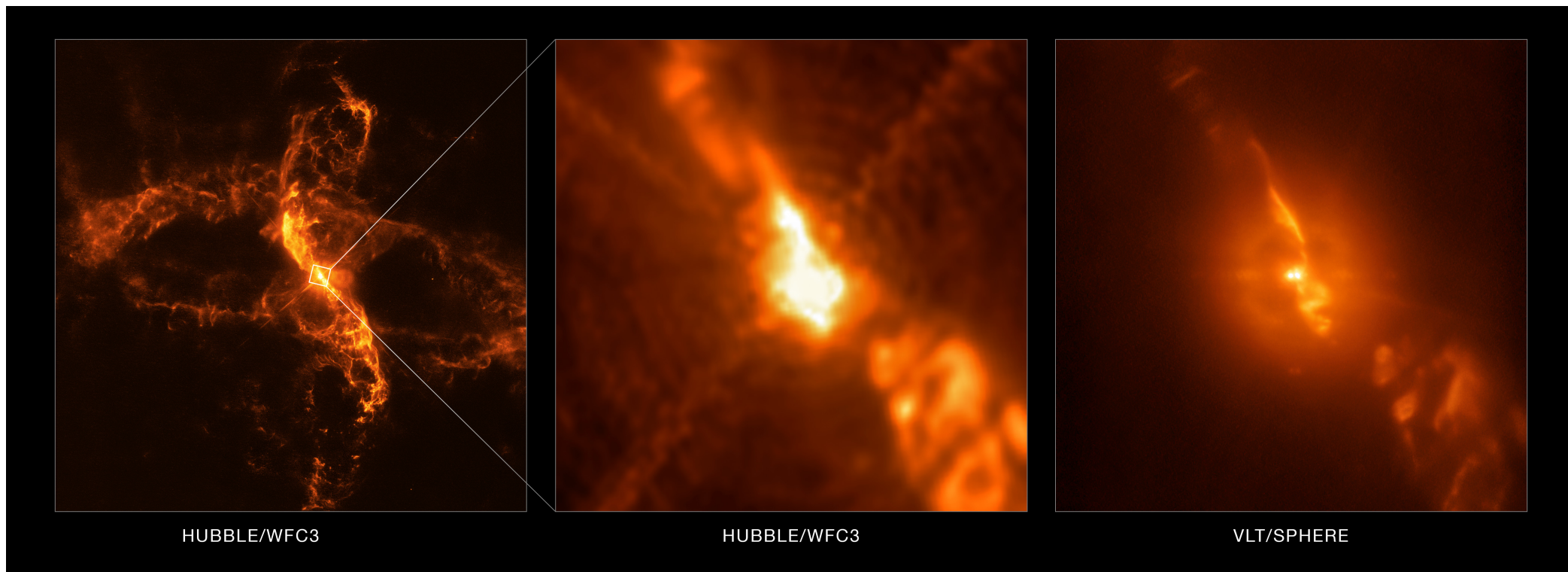
- Merrill 1921: bright nebular lines superposed on Md spectrum typical for LPVs
- Michalitsianos et al., 1980 :
 - Dense compact nebula,
 - Warm chromosphere
 - Secondary identified as white dwarf
- Wallerstein & Greenstein 1980: Reddening 0.67 in (B-V), $A_V \sim 2$
- Willson et al. 1981:

Mira component in the system being eclipsed by an extended gas cloud around the secondary star

Orbital period 44 years, duration 8.5 yr (20% of period). Next eclipse: 2018-2026

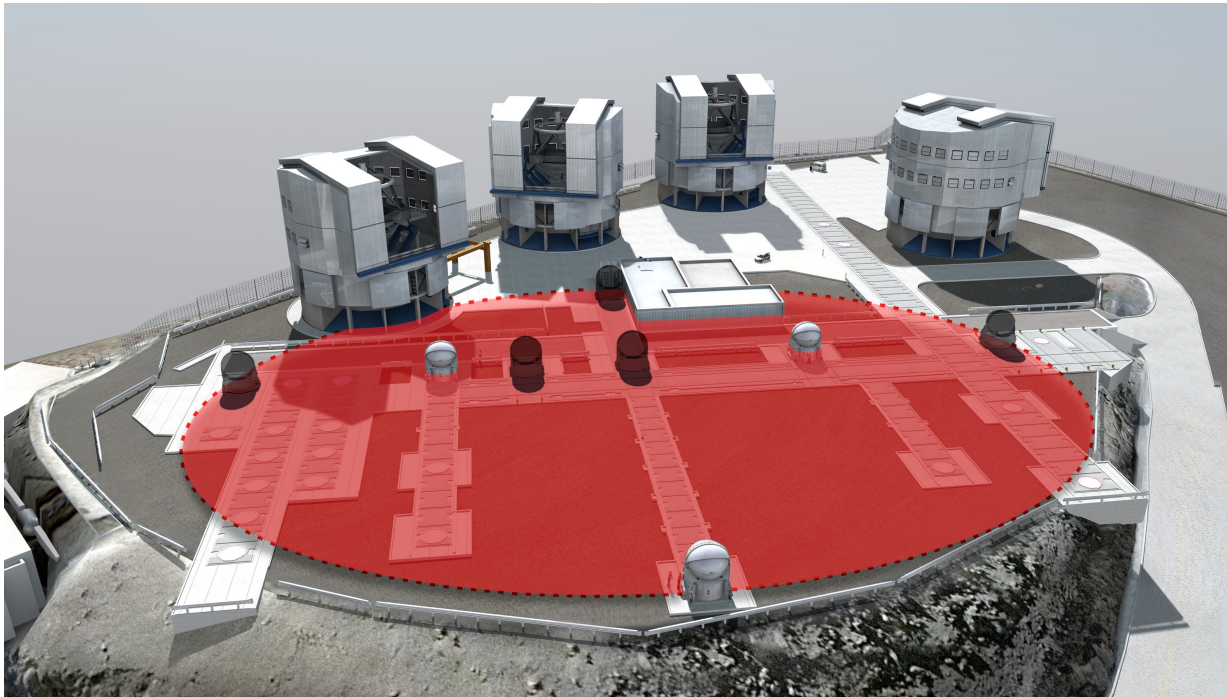
- Hinkle et al. 1989: Orbit with 44yr period and high eccentricity ($e=0.6$). All mass loss Mira forced through the Roche lobe onto the accretion disk of the secondary.
- Gromadzki & Mikolajewska 2009 : Refined orbit, period 43.6 yr, $e=0.25 \pm 0.07$, $M_{\text{tot}} 1.6-2.5 M_{\text{sun}}$, M_{h} (hot component)=0.6-1 M_{sun} ; M_{g} (giant)=1-1.5 M_{sun} ; mass ratio $q=M_{\text{g}}/M_{\text{h}}=1.2-2.1$.
- Min et al. 2014: Accurate parallax: 4.59 \pm 0.24 mas, distance 218 \pm 12/-11 pc





ESO/Schmid et al./NASA/ESA, <https://www.eso.org/public/images/eso1840b/>

VLT: A virtual 200-meter telescope



PIONIER:

H-band (1.5-1.7 μm), $R \sim 20$
Angular resolution up to ~ 1.5 mas

GRAVITY:

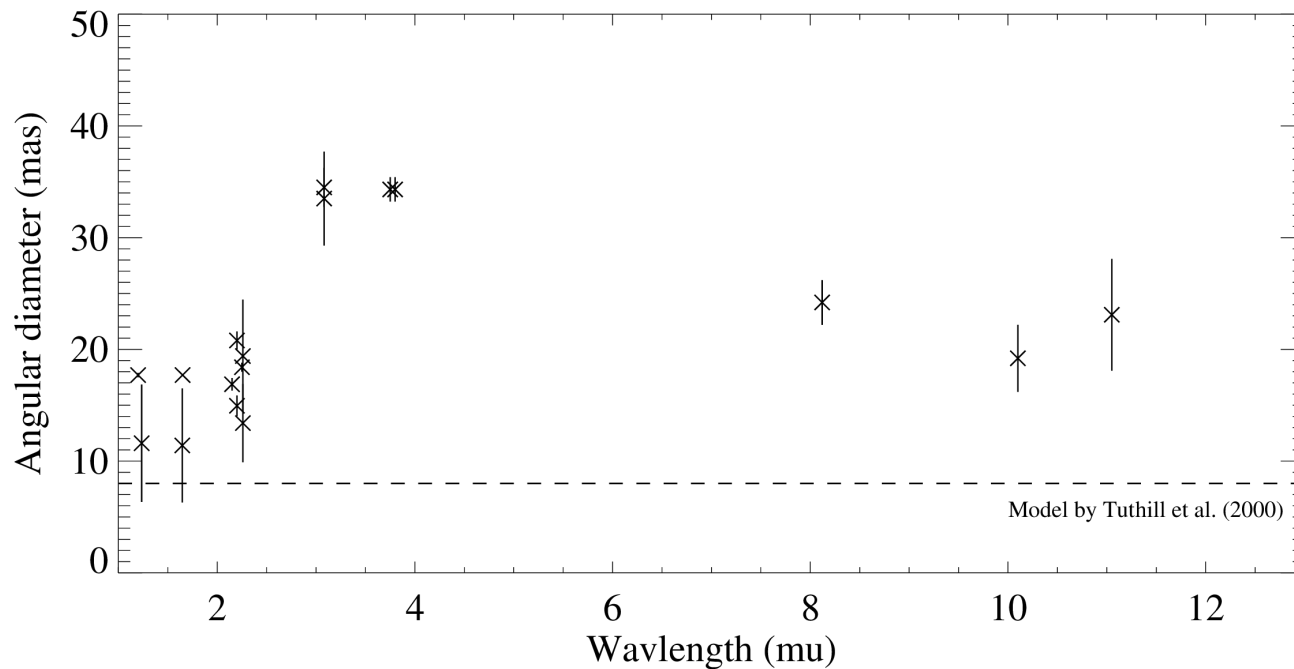
K-band (1.9-2.4 μm), $R \sim 22, 500, 4000$
Angular resolution up to ~ 2.2 mas

MATISSE:

LM-bands (2.8-4.1 μm), $R \sim 30, 500, 1000, 3500$
Angular resolution up to ~ 4 mas

N band (8-13 μm), $R \sim 30, 220$
Angular resolution up to ~ 10 mas

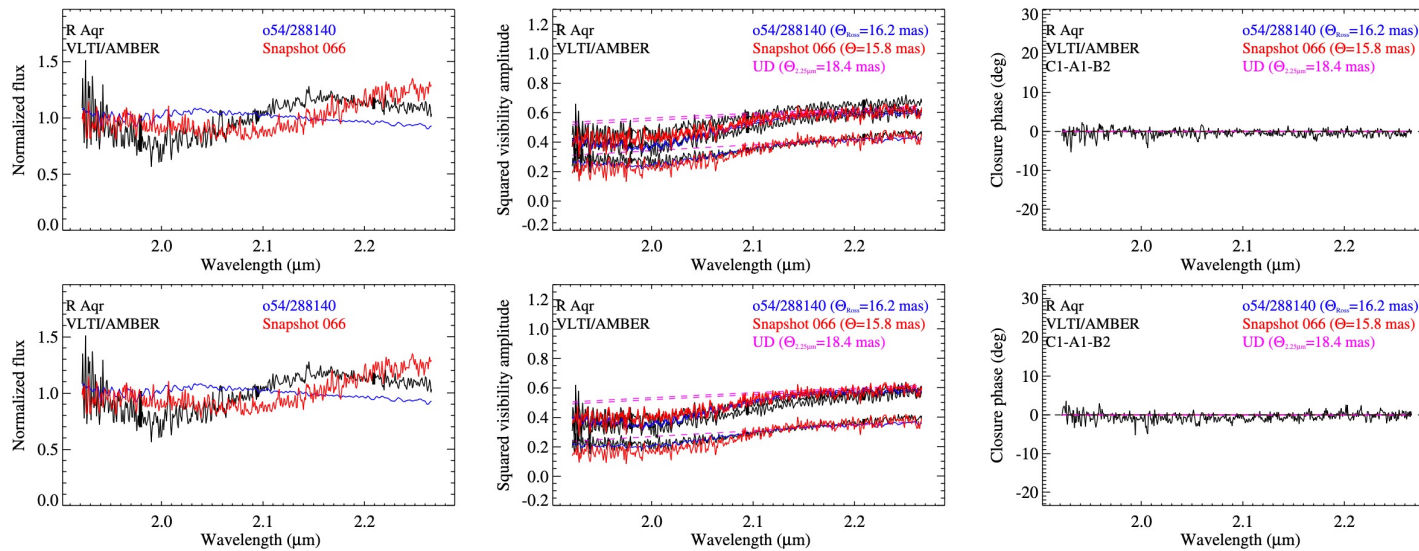
R Aqr angular diameters from the literature



- Near-continuum bands at 1.6 μm or 2.25 μm typically a good indicator of the photospheric diameter, while many other bands are contaminated by extended molecular layers (H₂O, CO, SiO)
- R Aqr: Larger than typical discrepancies between H and K near-continuum angular diameters

Van Belle et al. (1996), Tuthill et al. (2000), Chagnon et al. (2002), Mennesson et al. (2002), Millan-Gabet et al. (2005), Ragland et al. (2008), Zhao-Geisler et al. (2012), Wittkowski et al. (2016)

VLT/AMBER interferometry of R Aqr (10/2012)



	o Cet	R Leo	R Aqr	R Cnc	X Hya	W Vel
Phase	0.1	0.6	0.6	0.3–0.5	0.7–0.9	0.9–1.1
$\Theta_{\text{UD}}^{2.25 \mu\text{m}}$ (mas) ^a	28.5 ± 1.5	29.6 ± 1.3	18.4 ± 0.4	13.2 ± 0.3	6.0 ± 0.3	7.4 ± 0.2
m_{bol} (mag) ^b	1.04 ± 0.1	0.75 ± 0.1	2.37 ± 0.1	2.83 ± 0.4	4.00 ± 0.2	3.55 ± 0.2
Parallax (mas)	9.1 ± 1.4^c	10.0 ± 1.5^c	4.59 ± 0.24^d	3.6 ± 0.5^c	2.3 ± 0.3^c	2.0 ± 0.3^c
R (R_{\odot})	340 ± 80	320 ± 70	431 ± 33	400 ± 70	280 ± 60	400 ± 80
T_{eff} (K)	2450 ± 120	2570 ± 120	2250 ± 76	2390 ± 260	2700 ± 195	2700 ± 160
$\log L/L_{\odot}$	3.57 ± 0.27	3.60 ± 0.25	3.63 ± 0.12	3.66 ± 0.35	3.58 ± 0.28	3.88 ± 0.26

Wittkowski et al. 2016

New VLTI Observations of R Aqr

PIONIER

2019, July to August, Phase ~ 0.1

Imaging

GRAVITY

2016, October, Phase ~ 0.4

2018, August, Phase ~ 0.16

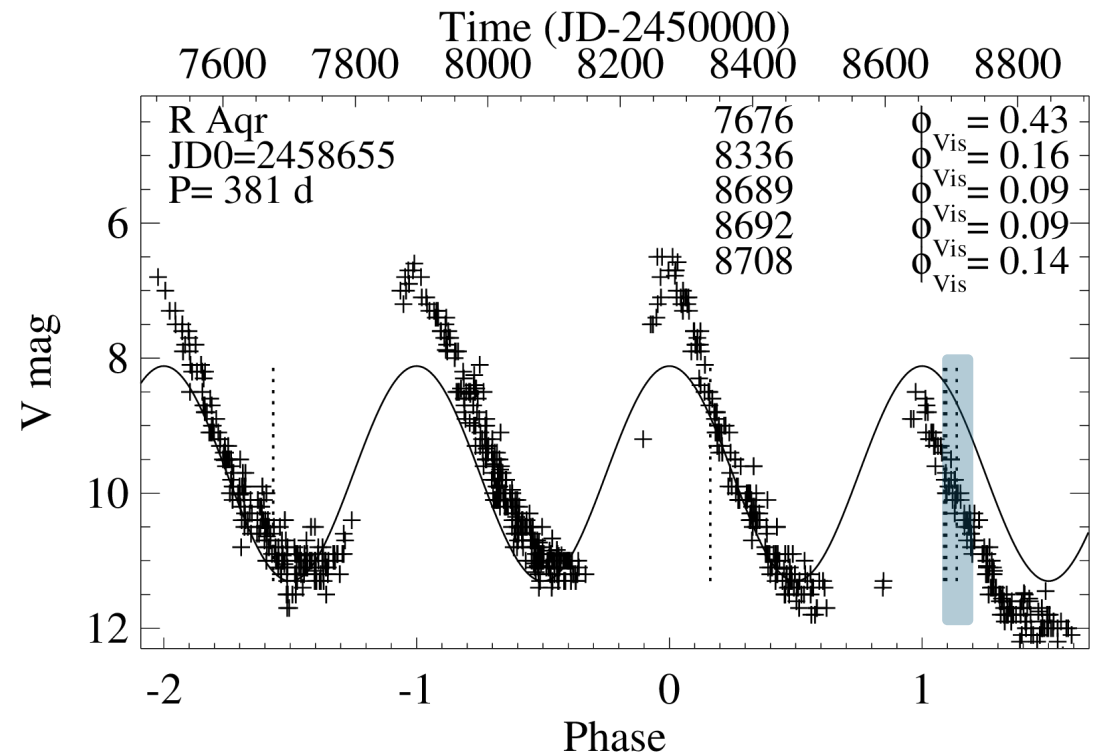
2019, August-September, Phase $\sim 0.1-0.2$

Snapshots

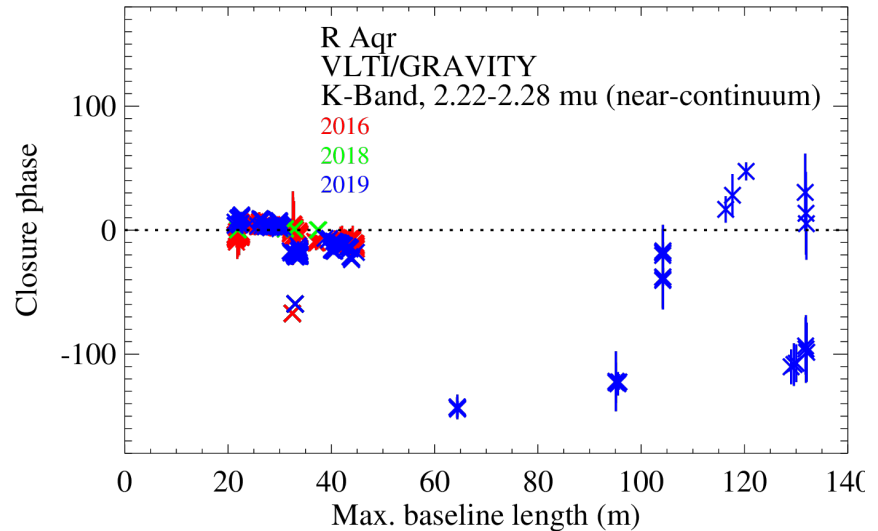
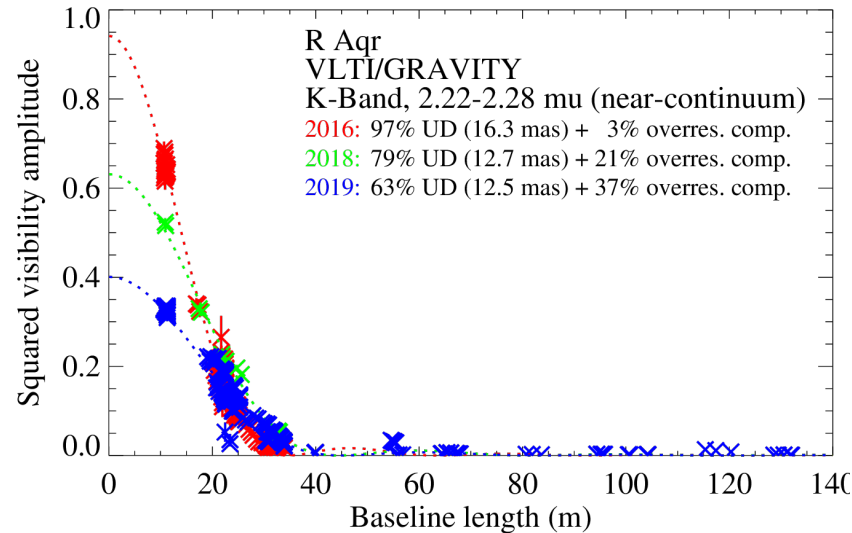
MATISSE:

2019, July to August, Phase ~ 0.1

Imaging



GRAVITY (near-IR K-band) results



Increasing contribution by an uncorrelated background component in the FOV (~ 0.25 arcsec):

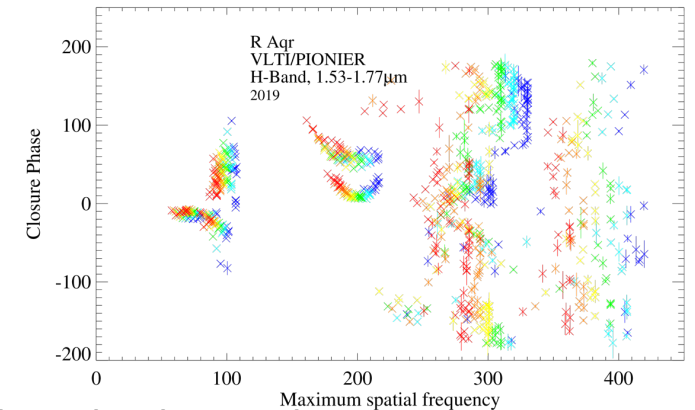
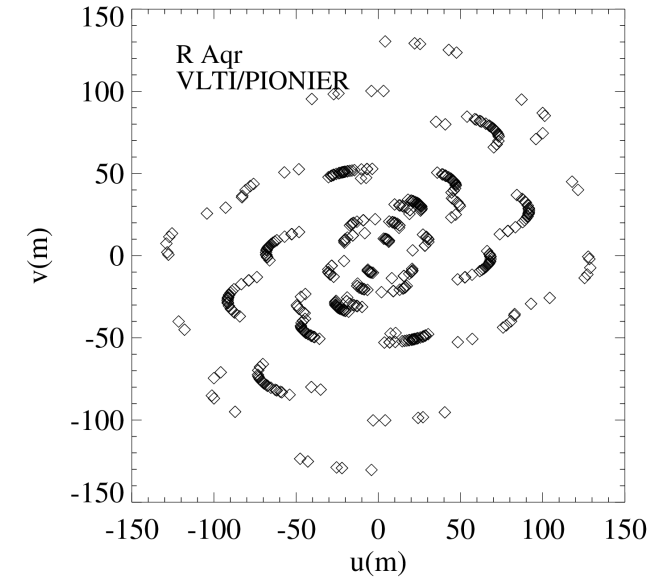
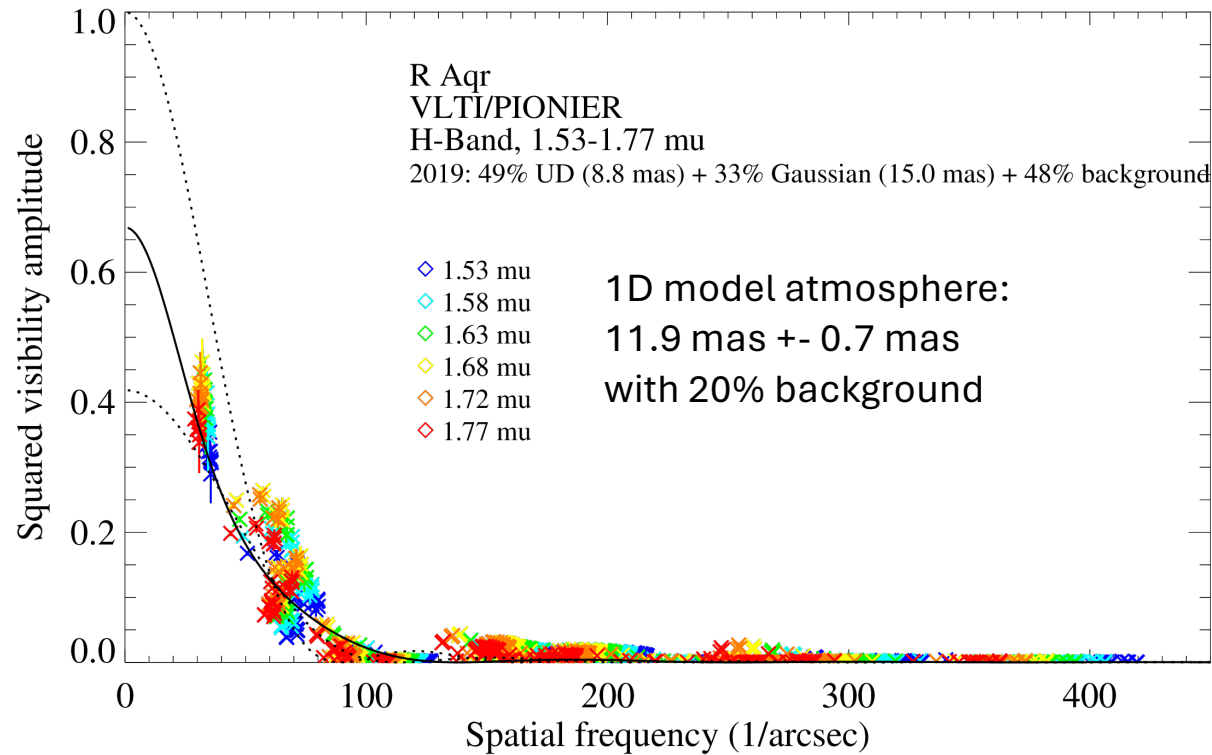
2016, before the suppression: 97% of the K-band continuum flux in the stellar (UD) component
 2018, early in the suppression: 79% of the K-band continuum flux in the stellar (UD) component
 2019, in the suppression: 63% of the K-band continuum flux in the stellar (UD) component

Continuum angular diameters in 2016 (phase 0.43), 2018 (0.16), 2019 (0.12):

16.3 mas , 12.7 mas , 12.5 mas

Pre-suppression epoch consistent with 2012 AMBER result (18.4 mas at phase 0.6).

PIONIER (near-IR H-band results)

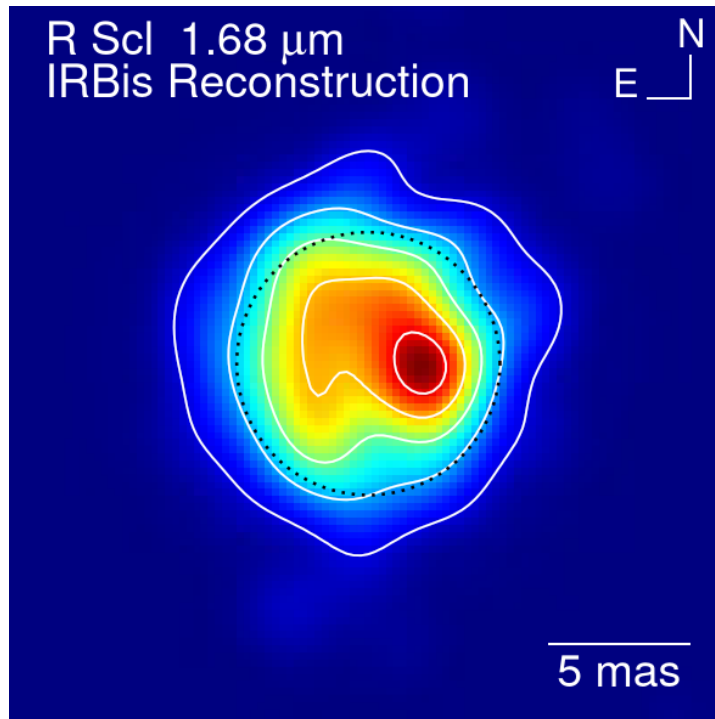


During the suppression event in 2019:

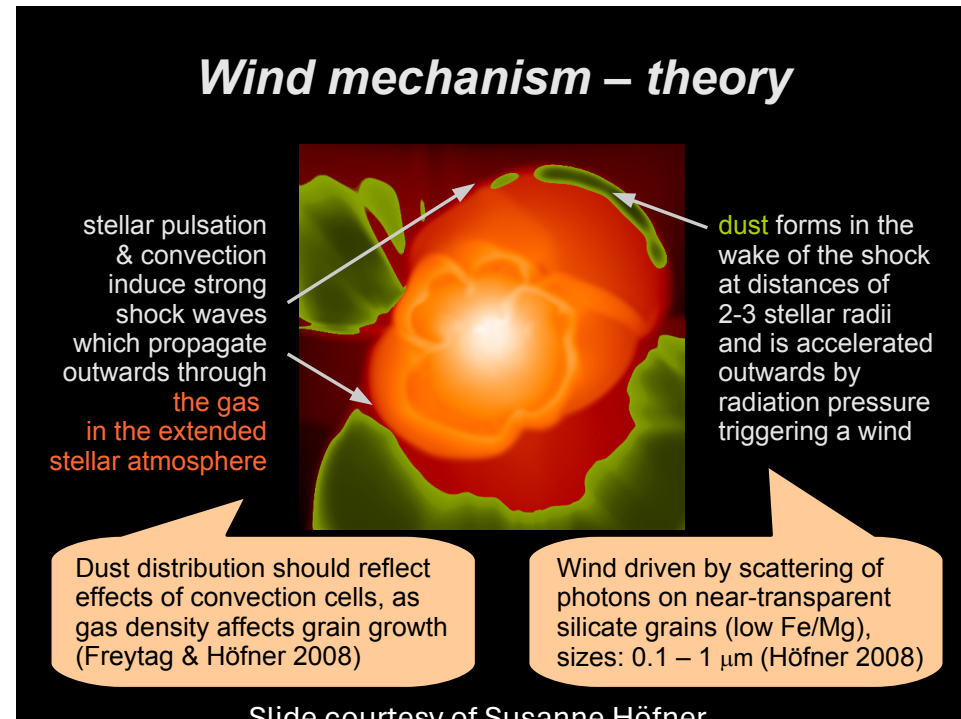
20-50% of the H-band flux in the FOV (~ 0.2 arcsec) from an uncorrelated large background component.

Angular diameter lower than obtained from GRAVITY, and much lower than previous estimates.

Resembling the carbon star R Scl observed with PIONIER



Wittkowski et al. 2017



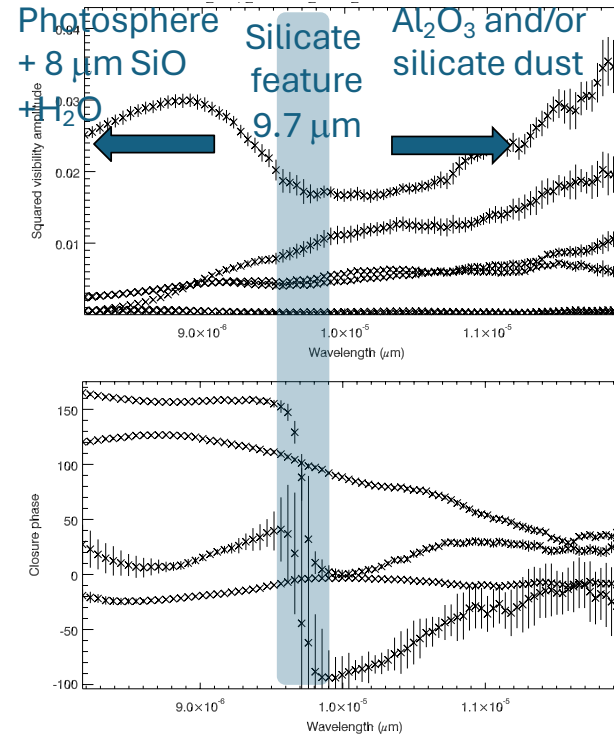
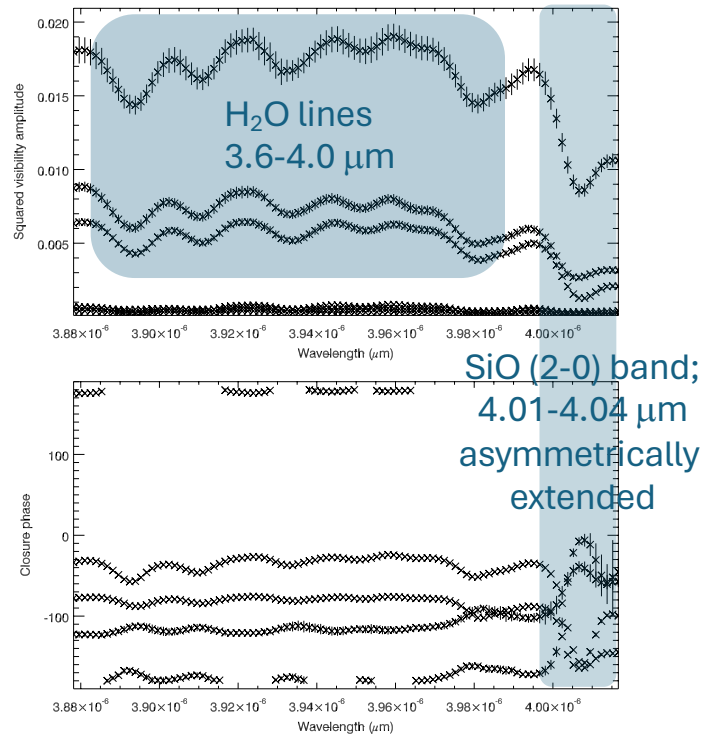
Interpretation of the image:

- (1) Giant convection cells resulting in large-scale shock fronts, leading to clumpy molecule and dust formation.
- (2) Dust clumps (amC) at radii of 2-3 R_{star} seen against the photosphere

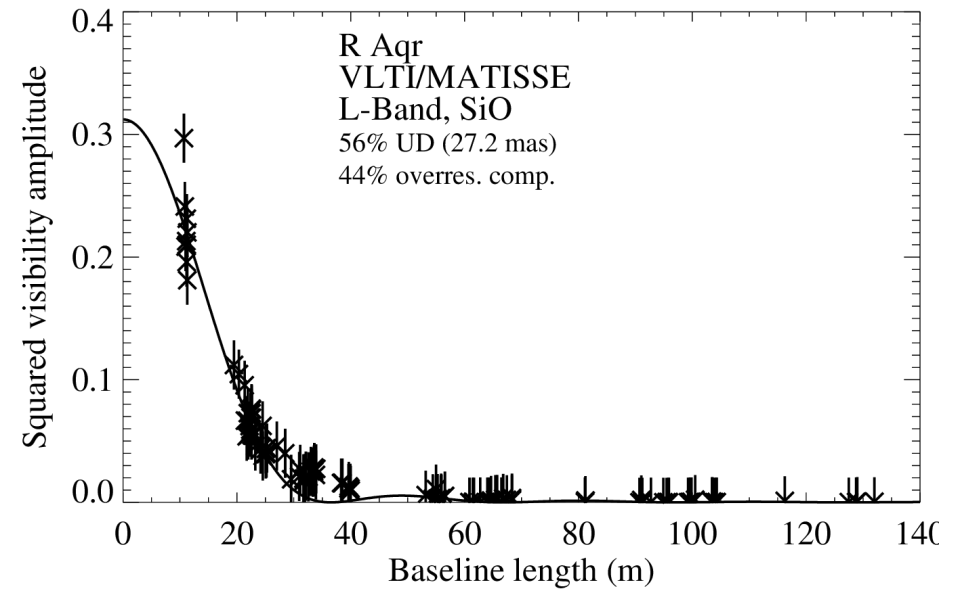
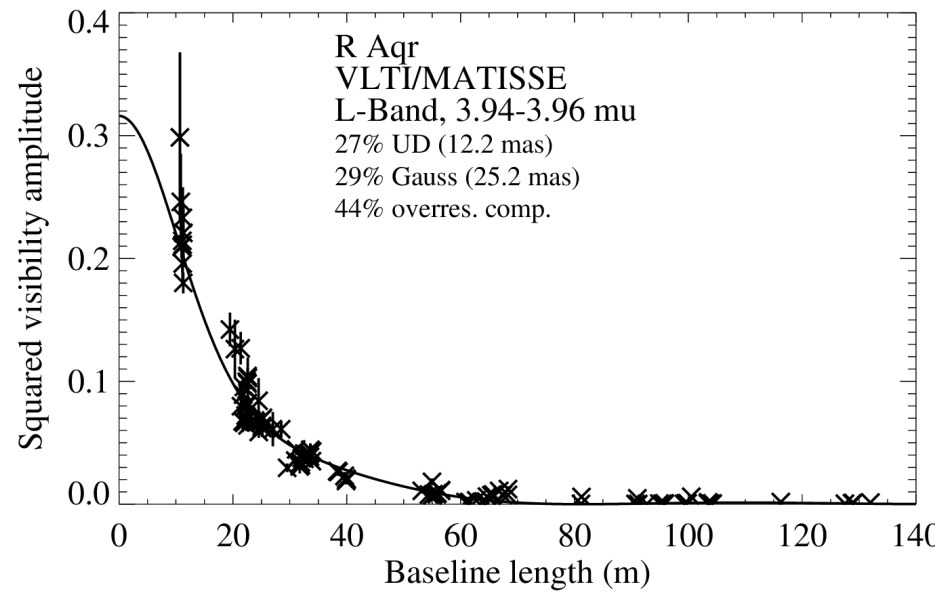
MATISSE (thermal IR LMN bands) results

L-band medium spectral resolution,
center $3.95\mu\text{m}$

N-band low spectral resolution

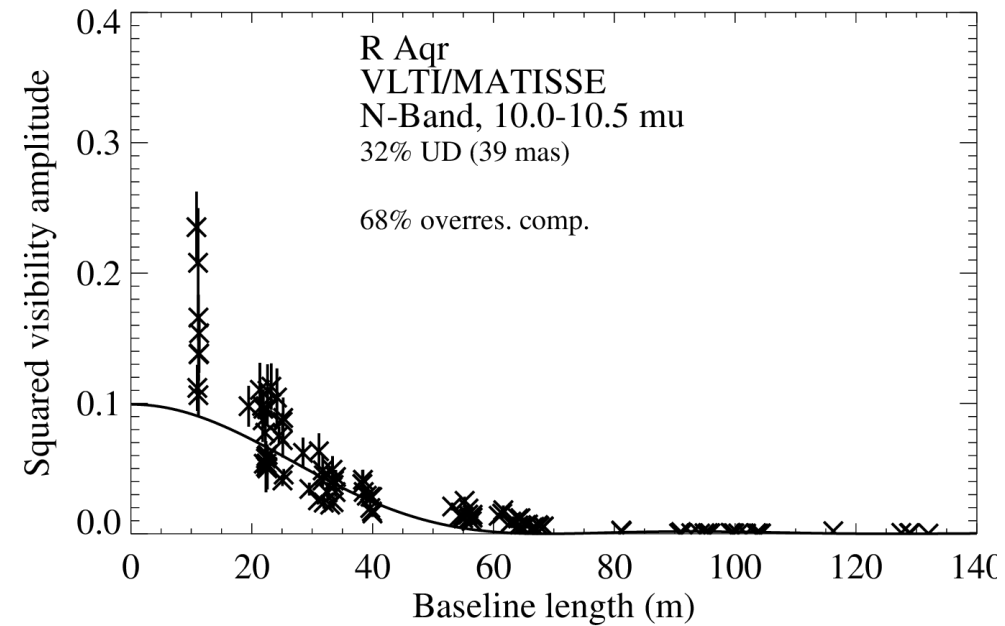
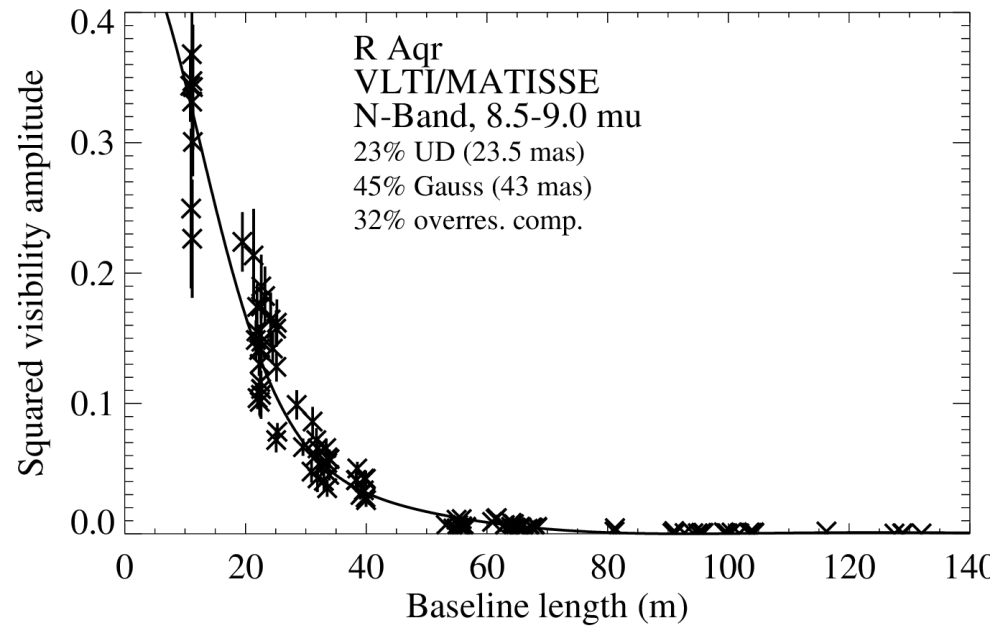


MATISSE L-band results



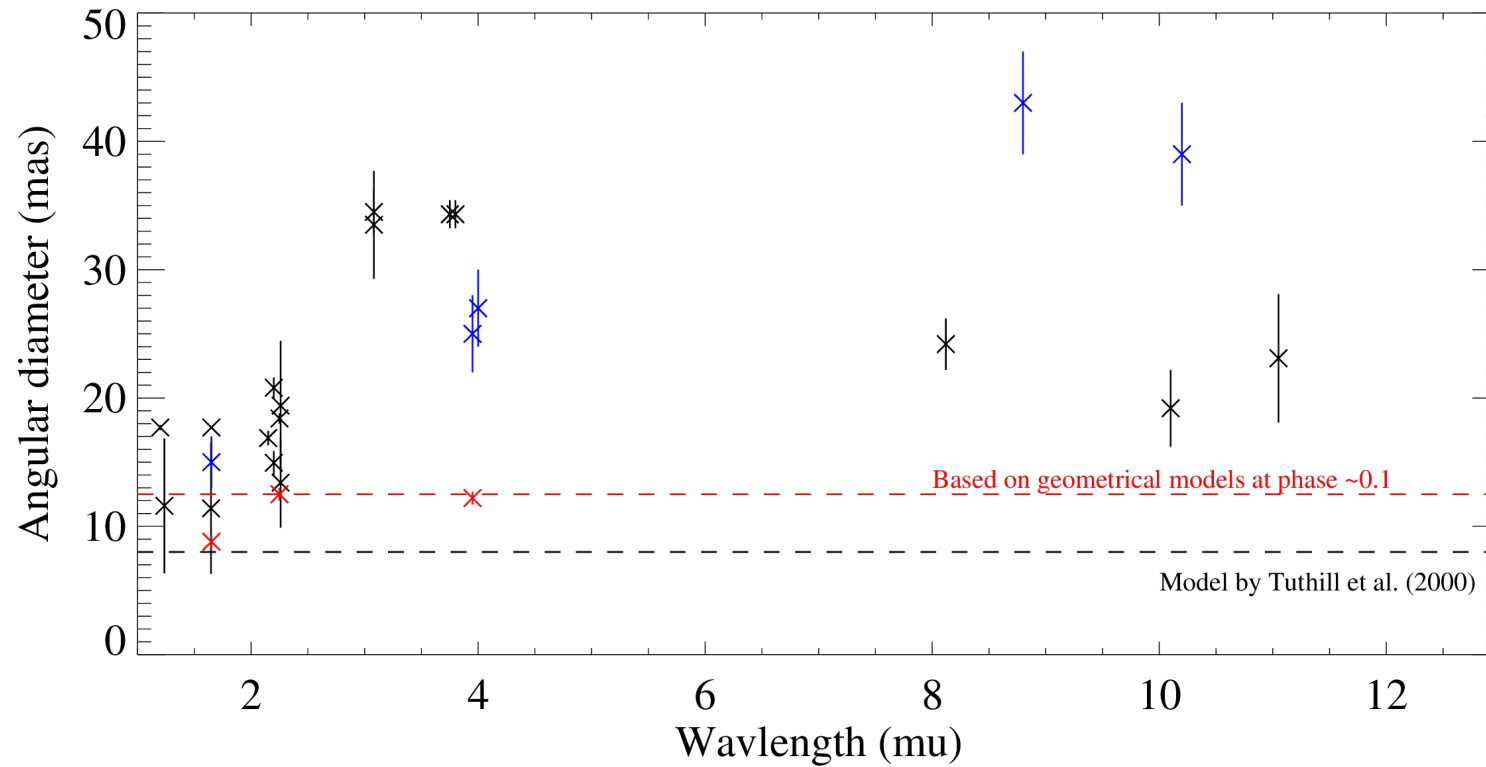
1D model atmosphere:
13.1 mas \pm 0.2 mas
with 42% background flux

MATISSE N-band results



Resolved structure confined within Roche lobe diameter of ~ 40 mas

Summary of angular diameters



Angular diameter overestimated in the past?

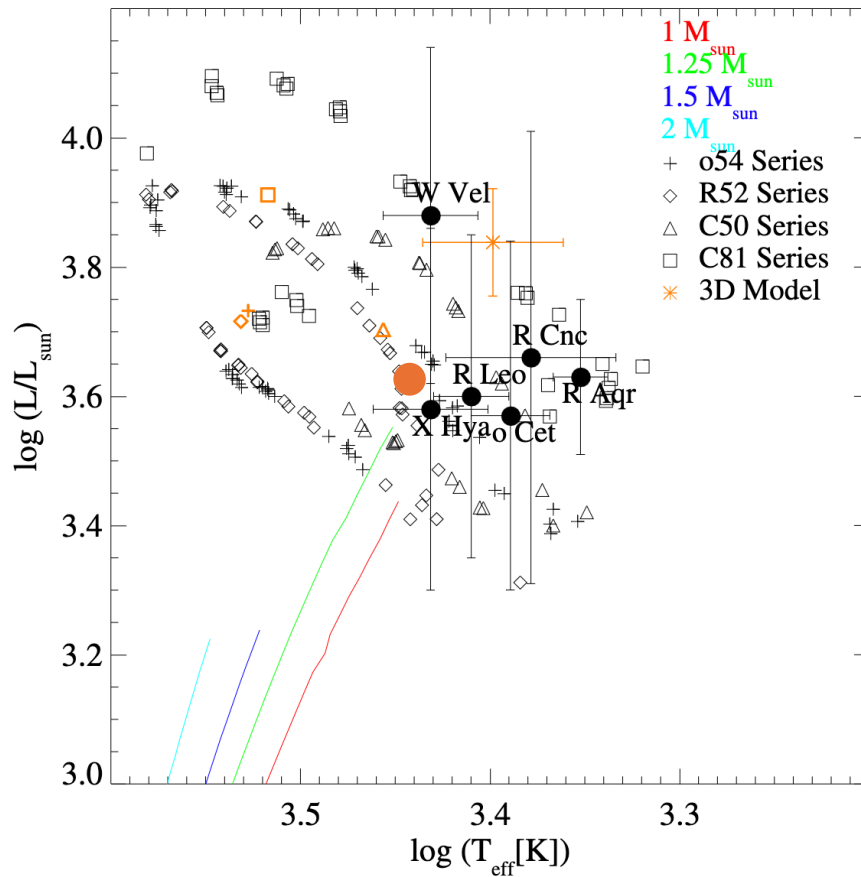


Figure from Wittkowski et al. 2016
 based on an angular photospheric diameter
 of 18.4 ± 0.4 mas at phase 0.6.

Angular diameter of 12.5 ± 0.5 mas:
 Radius: $431 \pm 33 R_{\text{sun}}$ \Rightarrow $293 \pm 30 R_{\text{sun}}$
 Teff: 2250 ± 76 K. \Rightarrow 2728 ± 120 K
 $\log(T_{\text{eff}})$: 3.48. \Rightarrow 3.44 ●

Summary

- Increasing contribution from an uncorrelated large background flux contribution at 2.2 μ : 3% in 2016, 20% in 2018, 50% in 2019
- Spatially resolved images of the Mira component in the near-IR H and K bands and the thermal-IR L, M, N bands
- H-band image seen behind foreground extinction
- Untypically large discrepancies of measured angular diameters in near-continuum bands
 - Angular photospheric diameters may be overestimated
 - Unusually strong contribution from the CSE
- No indication of mass transfer in the current image reconstructions